https://doi.org/10.5607/en21022
Exp Neurobiol. 2021 Aug;30(4):285-293.
pISSN 1226-2560 • eISSN 2093-8144

Original Article

Experimental Neurobiology

Region-Specific Differences in the Apoe4-dependent Response to Focal Brain Injury

Sung Eun Lee[1,2†], Haijie Yang[3†], Youngjun Sung[4], Younghoon Kim[1] and Sun Ah Park[1,2,5*]

[1]Lab for Neurodegenerative Dementia, Department of Anatomy, Ajou University School of Medicine, [2]Neuroscience Graduate Program, Department of Biomedical Sciences, Ajou University Graduate School of Medicine, [3]Department of Pharmacology, Ajou University School of Medicine, [4]Department of Biological Science, Ajou University, [5]Department of Neurology, Ajou University School of Medicine, Suwon 16499, Korea

Apolipoprotein E (apoE) plays a role in various physiological functions including lipid transport, synaptic plasticity, and immune modulation. Epidemiological studies suggest that the apoE4 allele increases the risk of post-traumatic sequelae. This study was performed to investigate region-specific effects of the apoE4 isoform on post-traumatic neurodegeneration. Two focal brain injuries were introduced separately in the motor cortex and hippocampus of apoE4 knock-in, apoE3 knock-in, apoE knockout, and wild-type (WT) mice. Western blotting showed that the expression levels of pre-synaptic and post-synaptic markers at the recovery stage were lower in the hippocampal injury core in apoE4 mice, compared with apoE3 and WT mice. Fast glial activation (determined by immunohistochemistry with glial fibrillary acidic protein, ionized calcium binding adaptor molecule 1, and cluster of differentiation 45 antibodies) was characteristic of apoE4 mice with hippocampal injury penumbra. apoE4-specific changes were not observed after cortical injury. The intensity of microglial activation in the hippocampus was inversely correlated with the volume of injury reduction on sequential magnetic resonance imaging examinations, when validated using matched samples. These findings indicate that the effects of the interaction between apoE4 and focal brain damage are specific to the hippocampus. Manipulation of inflammatory cell responses could be beneficial for reducing post-traumatic hippocampal neurodegeneration in apoE4 carriers.

Key words: Apolipoprotein E4, Neuroglia, Hippocampus, Inflammation, Brain injuries, Neurodegeneration

INTRODUCTION

Apolipoprotein E (apoE) is involved in lipid transport and cholesterol metabolism [1]. However, the presence of the apoE4 allele causes dysregulation of the lipid transport system, compared with non-apoE4 alleles [2]. apoE4 affects neuronal repair and remodeling in response to brain disorders [3]. Many epidemiological studies have suggested increased cognitive decline and delayed recovery after head trauma in patients with the apoE4 allele [4, 5]; however, the results have been inconsistent [6]. Animal studies that control for confounding factors have attempted to elucidate the role of the apoE4 isoform in the response to brain injury. Most of these studies have used transgenic mice that overexpress human apoE in an endogenous gene-deleted background [7, 8]. In recent years, a physiological model of apoE knock-in (KI) mice [9] has been studied [10-13]. These mice showed increased inflammation with neurodegeneration after focal penetrating injury [12] and blast injury [13]. However, in response to single cortical impact, the differential effects of apoE4 cannot be clearly validated [11]. Region-dependent differences in susceptibility to apoE4 effects might contribute to the inconsistent results.

To directly compare the region-specific effects of the apoE4 isoform, we introduced two focal brain injuries by injection of adenosine triphosphate (ATP) [14] into the mouse motor cortex and

Submitted June 23, 2021, Revised July 16, 2021,
Accepted August 4, 2021

*To whom correspondence should be addressed.
TEL: 82-31-219-5030, FAX: 82-31-219-5039
e-mail: sap001@ajou.ac.kr
†These authors contributed equally to this article.

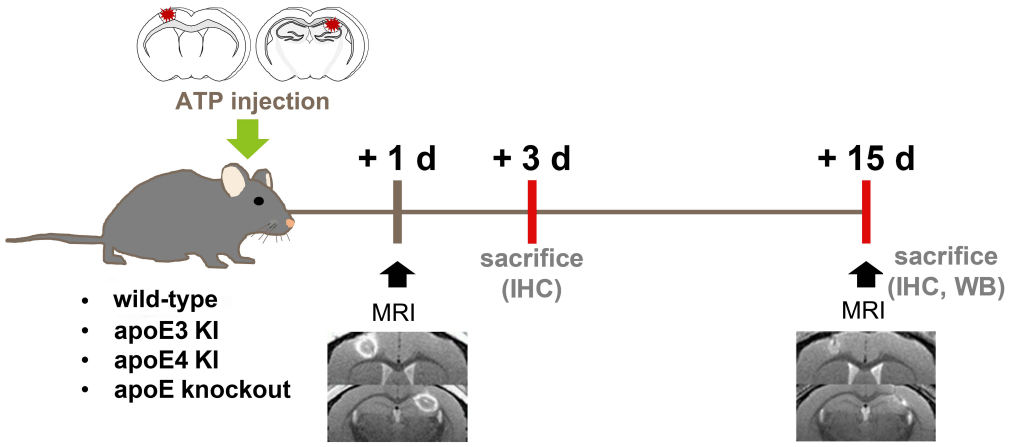

Fig. 1. Experimental flow. MRIs were taken on days 1 and 15 post-injury. Tissue was prepared on days 3 (n=19) or 15 (n=36) after ATP injection for immunohistochemistry and western blot. IHC, immunohistochemistry; KI, knock-in; WB, western blot.

hippocampus.

MATERIALS AND METHODS

Animals

ApoE 3KI, apoE 4KI [15], and apoE knockout (KO) [16] mice were purchased from Jackson Laboratory (#029018, #027894, and #002052, respectively). Mice were housed under a 12-h light/dark cycle with free access to food and water. The homozygotes of 3KI (f=8, m=6), 4KI (f=8, m=5), KO (f=6, m=8), and wild-type (WT) littermates (f=7, m=7) were used at age 20~24 weeks. All experiments were performed in accordance with protocols approved by the Ajou University Institutional Animal Care and Use Committee (2019-0045).

Stereotactic surgery

Focal brain injury was established through stereotactic injection of 0.8 μl ATP solution (500 mM), a well-known damage-associated molecular pattern [14]. The left motor cortex (M1, AP, +1.0; ML, +1.6; DV, -1.1) and right CA1 of the hippocampus (AP, -1.7; ML, -1.1; DV, -1.3) were selected for ATP injection.

Magnetic resonance imaging

Brain damage was evaluated at 1 and 15 days after injection by magnetic resonance imaging (MRI) of the brain at Sungkyunkwan University (Suwon, Korea). Mice were anesthetized with 1.5% isoflurane during MRI, and respiration and body temperature were continuously monitored. All MRI scans were performed on the horizontal bore 9.4 T/30 cm Bruker BioSpec magnetic resonance system (Billerica, MA, USA). T_2-weighted images were obtained by means of rapid acquisition using a refocused echoes sequence with the following parameters: repetition time/echo time=4,000/26 ms, rapid acquisition with refocused echoes factor=8, number of excitations=5, field of view=20 (readout)×20 (phase encoding) mm^2, matrix=256×256, in-plane resolution=78×78 μm^2, slice thickness=250 μm, and 30 contiguous slices without gap in the coronal plane. The images were saved in 124-kB TIFF format to measure damage volume in three dimensions using Mimics software (Materialise, Leuven, Belgium). Injury volume reduction in mice was validated using the following equation: (injury volume at 1 day – volume at 15 day)/injury volume at 1 day.

Tissue preparation

On days 3 (n=19) or 15 (n=36) after ATP injection (Fig. 1), mice were anesthetized and transcardially perfused with phosphate-buffered saline, then their brains were collected. For immunostaining, brains from 3KI (n=11), 4KI (n=9), KO (n=11), and WT (n=10) mice were post-fixed for 24 h in 4% paraformaldehyde and transferred to a 30% sucrose solution until the brains sank. Brains were then frozen in cooled isopentane, coronally sectioned (35 μm thickness) using a cryostat, and stored in an anti-freeze stock solution (phosphate buffer containing 30% glycerol and 30% ethylene glycol, pH 7.2) at -20℃ until analysis by free-floating immunostaining. ATP injection sites in the brain tissue block (0.2×0.2×1 mm^3) were isolated from the phosphate-buffered saline-perfused brains of 3KI (n=3), 4KI (n=4), KO (n=3), and WT (n=4) mice using the Alto Mouse Brain Slicer Matrix (Roboz Surgical Instruments, Gaithersburg, MD, USA). Tissue blocks from matching regions were obtained from uninjured mice (n=1 per genotype). The tissues were stored at -80℃ until use.

Immunohistochemistry and microscopy

Three consecutive sections with 210-μm intervals were used for immunohistochemistry. The cryosections were permeabilized with Tris-buffered saline, 0.2% Triton X-100 (TBST) for 20 min. Sections were subsequently blocked in 5% serum in TBST, fol-

https://doi.org/10.5607/en21022

Table 1. Used antibodies in this study

Antibodies	Dilution factors for	
	Western blot	Immunostaining
Mouse anti-PSD95 (abcam, ab2723)	1:2,000	
Mouse anti-gapdh (Santacruz, sc32233)	1:2,000	
Rabbit anti-GFAP (Sigma, G9269)		1:500
Rabbit anti-NeuN (Millipore, ABN78)	1:2,000	
Rabbit anti-Iba-1 (Wako, 019-19741)		1:1,000
Rabbit anti-synaptophysin (abcam, ab32127)	1:5,000	
Rat anti-CD45 (Mybiosource, MBS520149)		1:1,000
Donkey anti-mouse IgG, Alexa Fluor 488 (Thermo Fisher scientific, A-21202)		1:500
Donkey anti-mouse IgG, Alexa Fluor 647 (Thermo Fisher scientific, A-31571)		1:500
Donkey anti-rabbit IgG, Alexa Fluor 647 (Thermo Fisher scientific, A-31573)		1:500
Donkey anti-rat IgG, Alexa Fluor 488 (Thermo Fisher scientific, A-21208)		1:500
Goat anti-mouse IgG (H+L) secondary antibody HRP (Thermo Fisher scientific, 31431)	1:20,000	
Goat anti-rabbit IgG (H+L) secondary antibody HRP (Thermo Fisher scientific, 31460)	1:20,000	

lowed by incubation with primary antibodies at 4℃ overnight and secondary antibodies at room temperature for 2 h. To minimize nonspecific fluorescence quenching in the damaged regions, sections were treated with 0.1% Sudan black B reagent in 70% ethanol for 20 min and washed with TBST. The images were captured by confocal laser scanning microscopy (K1-Fluo; Nanoscope Systems, Daejeon, Korea) and analyzed using ZEN software (Carl Zeiss, Oberkochen, Germany).

Damaged areas were visualized by bright-field microscopy after staining with Sudan Black B, which permitted line drawing to designate the injury core. Because injured tissues were torn or lost in many sections, immunohistochemical analysis was performed in the penumbra region of the injury. In the M1 injury, the penumbra region was defined to encompass the area that was ≤437 μm from the margin of the injury core, which corresponded to the field of view at 20× magnification. Two regions of interest were selected in the lateral and medial parts of the penumbra (437×437 μm^2 in each part) for image analysis. In the hippocampus, the penumbra was defined as the circumferential area ≤100 μm from the border of the injury core to include the hippocampus proper, avoiding the adjacent third ventricle in all examined sections; the medial part of the penumbra (100×200 μm^2) was chosen as the region of interest. To quantify cell type-specific markers, the positive cell number (neuronal nuclear protein [NeuN]) was counted using ImageJ software (version 1.53 g, NIH, Bethesda, MD, USA) and fluorescence intensity (glial fibrillary acidic protein [GFAP], ionized calcium binding adaptor molecule 1 [Iba-1], cluster of differentiation 45 [CD45], Iba-1/CD45-double positive [$Iba\text{-}1^+/CD45^+$]) was analyzed using ZEN software (Carl Zeiss).

Western blotting analysis

Frozen tissue blocks were thawed on ice, then incubated with 60~80 μl radioimmunoprecipitation assay buffer containing a protease inhibitor cocktail (Roche Diagnostics, Mannheim, Germany) and phosphatase inhibitor (Roche Diagnostics KK, Tokyo, Japan). Tissues were homogenized three times using a tissue grinder for 2 s each, then sonicated twice with an ultrasonic processor for 3 s each. After centrifugation at 13,000 rpm for 10 min at 4℃, the supernatant was incubated with sample buffer for 5 min at 95℃. Then, 20 μg protein was resolved by sodium dodecyl sulfate-polyacrylamide gel electrophoresis and electrotransferred to a polyvinylidene difluoride membrane. The membrane was blocked in 5% bovine serum albumin (Bovogen, VIC, Australia) and probed with the appropriate antibodies (Table 1). Proteins were detected by enhanced chemiluminescence (Advansta, Menlo Park, CA, USA) and quantified using ImageJ software.

Statistical analyses

All statistical analyses were performed using SPSS Statistics version 20 (IBM Corp., Armonk, NY, USA). Variables from MRI and immunohistochemistry analyses were normally distributed according to the Shapiro–Wilk test. Therefore, one-way analysis of variance followed by Tukey's post hoc test was used for group comparisons. $p<0.05$ was considered statistically significant. Western blotting data were obtained from a fewer number of samples and were not normally distributed. Therefore, nonparametric tests including the Kruskal–Wallis test and subsequent post hoc analyses using the Mann–Whitney test with multiple comparison correction by means of the false discovery rate method (false discovery rate<0.1) were used [17] for western blotting data. Correlation analyses were performed using Pearson's correlation test to identify significant interrelationships between data from immunohistochemistry and neuroimaging studies, and correlation coefficients (r) were obtained. $p<0.05$ was considered statistically significant.

RESULTS

Identification of focal brain damage using MRI

The location and volume of focal damage in the motor cortex and hippocampus were examined using sequential MRI on days 1 and 15 post-injury. Initial MRI demonstrated well-demarcated injuries, which were distinct from the intact brain, revealing T2-hyperintense rings containing mixed signals. The entire volume circled by T2-hyperintense signals was measured in three dimensions using Mimics software (Materialise) in all mice and was identified as the injury volume; this volume did not differ according to apoE genotype in both the cortex and hippocampus according to one-way analysis of variance (M1, p=0.144; CA1, p=0.662) (Fig. 2A). Follow-up brain MRIs were performed on day 15. The remaining areas of damage were much smaller and less intense than previous areas and the extents were comparable across all groups (M1, p=0.462; CA1, p=0.225) (Fig. 2B). The reduction in injury volume was estimated as the reduction of remaining injury

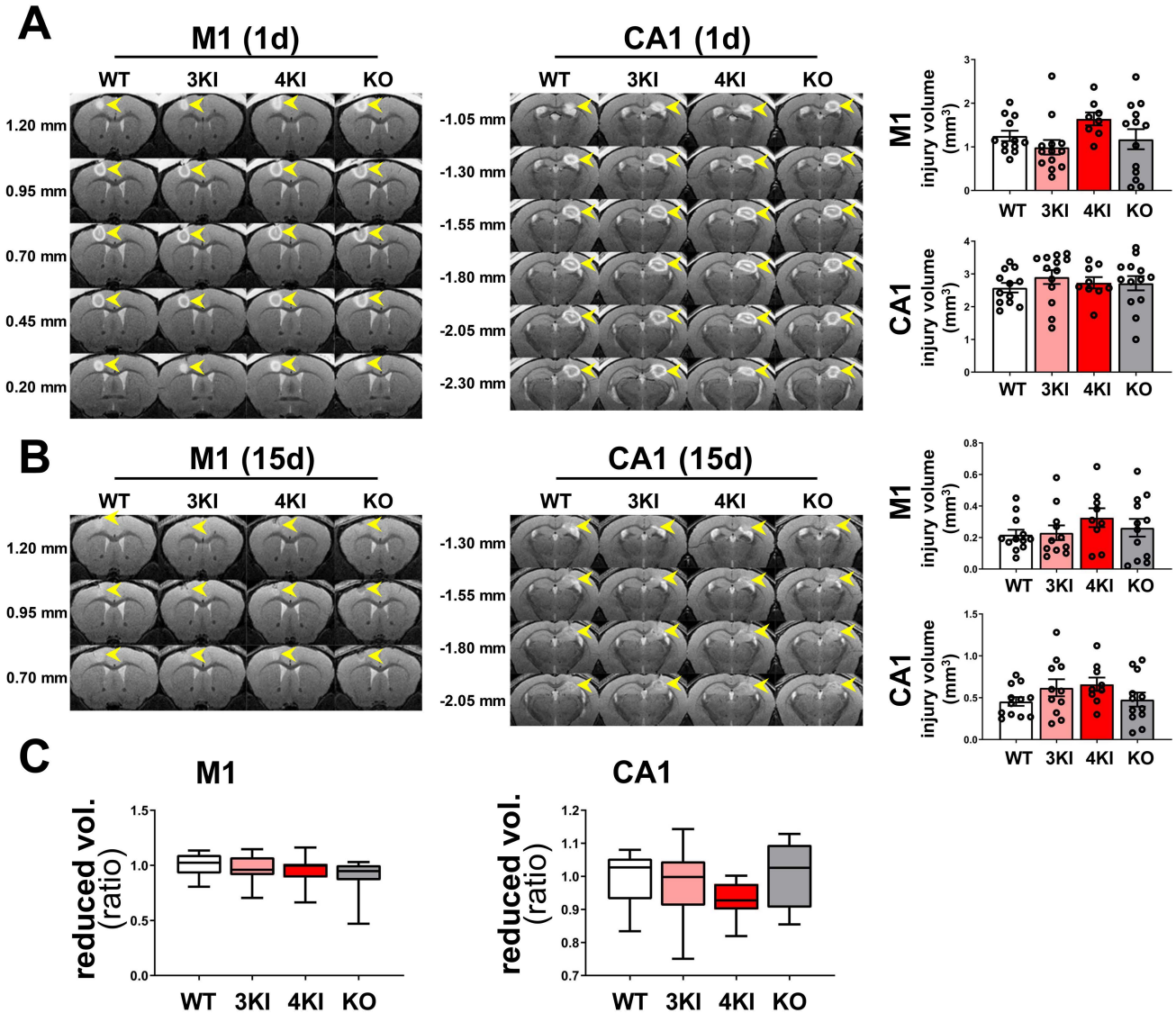

Fig. 2. Focal brain injury and its recovery on brain MRI. (A) MRI on day 1 after ATP injection showed well-demarcated focal injuries in the motor cortex (M1) and hippocampus (CA1) as T2-hyperintense signals (arrowheads). The volumes of injured tissue were comparable among apoE genotypes (all p>0.05). (B) Damaged regions were shrunken and magnetic resonance signals exhibited lower intensity on day 15. The volumes of remaining injuries were similar in all groups (all p>0.05). (C) Damage reduction on day 15, compared with day 1, did not differ in the cortex and hippocampus across all groups (all p>0.05). Bar graphs show means±standard errors of the mean. Box plots show medians and interquartile ranges, while whiskers represent maximum and minimum values. *p<0.05, significant on one-way analysis of variance with post hoc Tukey's test. 3KI, apoE3 knock-in; 4KI, apoE4 knock-in; KO, knockout; vol, volume; wt, wild-type.

https://doi.org/10.5607/en21022

from the initial damage volume in individual mice; this reduction was similar in all groups (M1, p=0.408; CA1, p=0.218) (Fig. 2C).

Lower synaptic protein levels in the hippocampus of 4KI mice during recovery

Western blotting analysis was conducted using tissue from 3KI (n=3), 4KI (n=4), KO (n=3), and WT (n=4) mice. Based on the volume of damage observed by MRI, the tissue blocks mainly contained the injury core. Immunoblotting using a NeuN antibody, a marker for neurons, did not reveal a significant difference according to apoE genotype (Fig. 3). However, the expression patterns of presynaptic (synaptophysin, SYP) and post-synaptic (post-synaptic density-95 [PSD-95]) proteins demonstrated region- and isoform-specific alterations. SYP levels in the motor cortex were lower in 3KI and 4KI mice than in WT mice (p=0.029), whereas PSD-95 levels did not differ across apoE groups. In contrast, a significant apoE4 isoform-dependent change was observed in the hippocampus. Both SYP and PSD-95 expression levels were significantly decreased in 4KI mice, compared with 3KI and WT mice (SYP, p=0.017; PSD-95, p=0.041); the extents of reduction were similar to the level of apoE deficiency. These data suggest that apoE4 expression inhibits apoE-dependent synaptic repair after focal injury in the hippocampus.

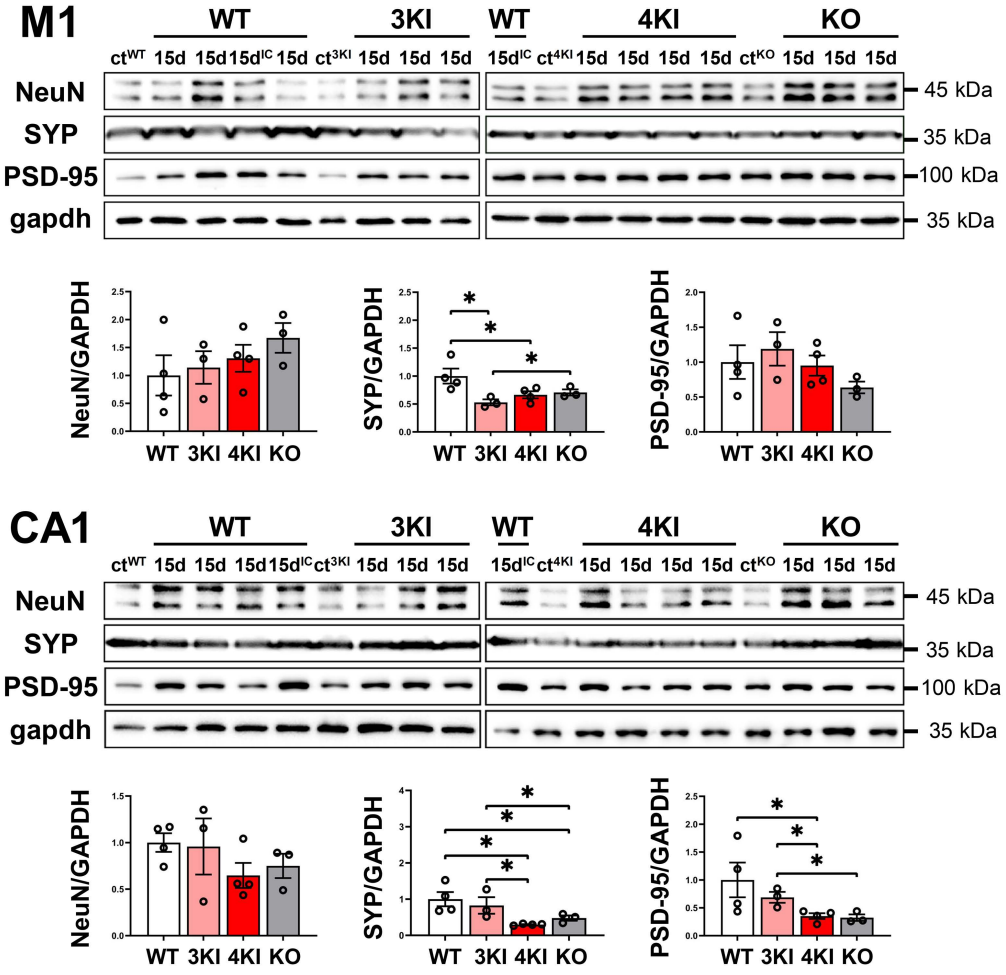

Fig. 3. Western blotting analysis of the injury core on day 15. Western blotting and densitometric analyses showed comparable NeuN expression levels in all groups in both the motor cortex (M1) and hippocampus (CA1) (p>0.05). The expression of SYP was significantly decreased upon cortical injury of 3KI and 4KI with respect to wild-type mice (p=0.029), whereas PSD-95 levels were equivalent. Both SYP and PSD-95 expression levels in the hippocampus showed isoform-dependent changes: significant reductions in 4KI and KO mice, compared with 3KI and wild-type mice (p=0.017 and p=0.041, respectively). Bar graphs show means±standard errors of the mean. *p<0.05, significant on Kruskal–Wallis test and subsequent post hoc analyses using the Mann–Whitney test with multiple comparison correction by means of FDR<0.1. 3KI, apoE3 knock-in; 4KI, apoE4 knock-in; ct, control mice without injury; IC, repeatedly loaded sample to compare two blots; KO, knockout; NeuN, neuronal nuclear protein; SYP, synaptophysin; PSD-95, postsynaptic density-95; wt, wild-type.

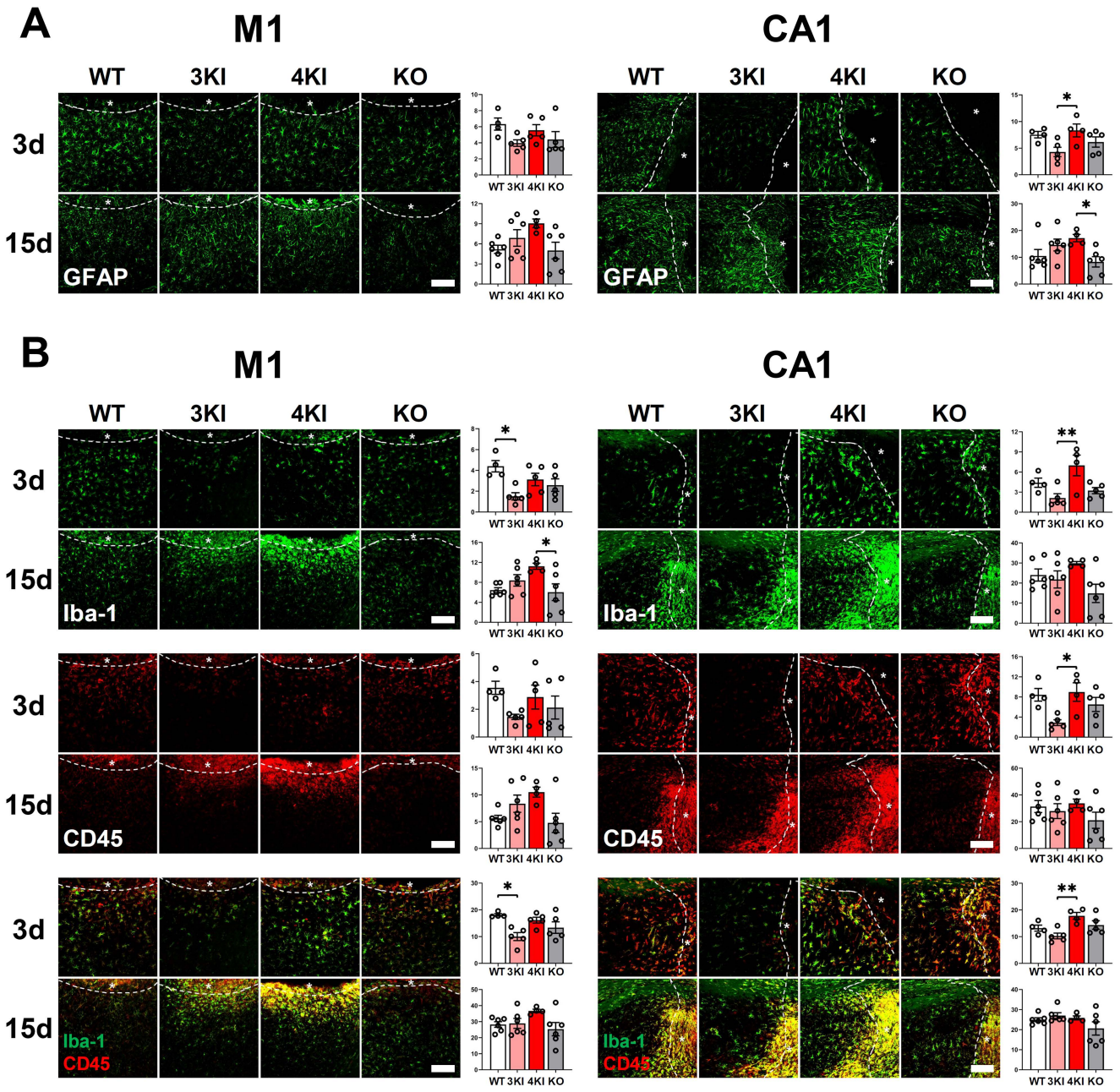

Fig. 4. Immunohistochemical assessment of glial markers and correlation analysis. (A) GFAP immunohistochemical assessment showed higher astrocytic activation upon hippocampal injury in 4KI mice, compared with 3KI mice on day 3 (p=0.042) and compared with KO mice on day 15 (p=0.048). (B) Iba-1$^+$ and Iba-1$^+$/CD45$^+$ signals were significantly lower in 3KI mice than in wild-type mice upon cortical injury on day 3 (p=0.016 and p=0.011, respectively), and the Iba-1$^+$ signal was higher in 4KI mice than in KO mice on day 15 (p=0.038). Iba-1, CD45, and Iba-1/CD45 immunoreactivities in the hippocampus were all higher in 4KI mice than in 3KI mice on day 3 (p=0.009, p=0.019, and p=0.009, respectively). These markers further elevated on day 15, although the group differences disappeared. (C) A significant inverse correlation between injury volume reduction on MRI and Iba-1 immunoreactivity (r=-0.434, p=0.049), and a tendency for inverse correlation between MRI marker and Iba-1$^+$/CD45$^+$ (r=-0.430, p=0.052), were identified in correlation analysis. The asterisks (*) in figures indicate the side of injury core. The dotted lines show the border of injury core. Bar graphs show mean±standard errors of the mean. Scale bar, 100 μm. *p<0.05 and **p<0.01, significant on one-way analysis of variance with post hoc Tukey's test (A, B) and Pearson's correlation analysis (C). γ, correlation coefficients; 3KI, apoE3 knock-in; 4KI, apoE4 knock-in; GFAP, glial fibrillary acidic protein; KO, knockout; wt, wild-type.

https://doi.org/10.5607/en21022

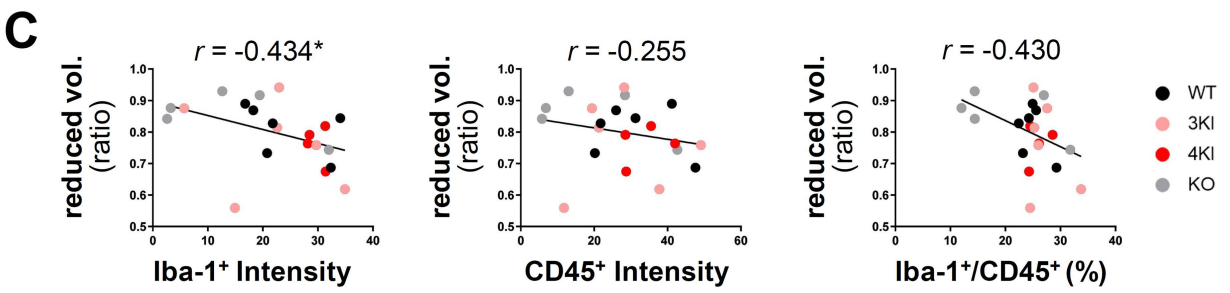

Fig. 4. Continued.

Early higher glial activation and monocytic infiltration in the hippocampus of 4KI mice

ApoE is primarily expressed and produced by astrocytes and microglia [1, 18]. Glia play key roles in injury repair and synaptogenesis [19]. To explore apoE isoform-specific effects on glia, immunohistochemistry was conducted with antibodies against astrocytes, microglia, and monocytes. The brain slices obtained on day 3 were additionally prepared to examine early changes. Enhanced astrocytic activation (indicated by increased GFAP signals) was observed in the hippocampus of 4KI mice, relative to 3KI (p=0.042; Fig. 4A). The discrepancy between apoE4 and apoE3 disappeared on day 15 with further enhanced astrocytic activities in both mice. The inflammatory markers validated by Iba-1 and CD45 immunohistochemistry demonstrated a pattern similar to the GFAP pattern in the hippocampus: apoE4-specific early increases (p=0.009 and p=0.019; Fig 4B), followed by comparably enhanced immunoreactivity in all groups on day 15. Upon cortical injury, no apoE isoform-dependent effect on microglial activities was observed. Only lower Iba-1 signals in 3KI mice than in WT mice on day 3 (p=0.016), and higher Iba-1 signals in 4KI mice than in KO mice on day 15 (p=0.038), were noted. To further characterize the microglial activation, we quantified monocyte conversion into microglia, which exhibit Iba-1+/CD45+ double positivity [20]. The results also demonstrated an apoE4-specific early increase in hippocampal injury.

Correlation analyses of glial activation and injury volume reduction

To explore the link between inflammatory cell activity in the penumbral area and injury recovery, correlation analyses were conducted. Immunohistochemistry was performed on day 15 in mouse brains for which follow-up MRI had been performed. Accordingly, these brains were used for correlation analyses. There were no significant relationships between the intensities of inflammatory cell markers and changes in injury volume in the cortex (Iba-1, r=0.174, p=0.452; CD45, r=0.165, p=0.475; Iba-1+/CD45+, r=0.169, p=0.463). However, Iba-1 (r=-0.434, p=0.049) and Iba-1+/CD45+ (r=-0.430, p=0.052) immunoreactivity upon hippocampal injury revealed a significant inverse correlation and a tendency toward an inverse correlation with injury recovery, respectively (Fig. 4C). Notably, monocyte ($CD45^+$) infiltration itself did not show a significant correlation (r=-0.225, p=0.328). These findings suggest that increased microglial activation is related to disrupted injury repair in the hippocampus.

DISCUSSION

The apoE4 allele is one of the most common and strongest risk factor genes in sporadic Alzheimer's disease (AD) [21], while traumatic brain injury is a potent environmental risk factor for AD [22]. The brain regions selected for the current study, namely the primary motor cortex and hippocampus, are most resistant and most vulnerable to neurodegeneration in AD, respectively [23, 24]. The differential effects of apoE4-brain injury interaction according to the brain region at least partly explain the differences in susceptibility to post-traumatic neurodegeneration and dementia, with respect to the apoE4 allele. In this study, we found lower synaptic protein expression in the injury core of the hippocampus during the recovery stage in apoE4 mice, compared with apoE3 mice. Faster and higher glial activation and monocytic infiltration with a higher conversion rate into microglia were characteristic responses to focal brain injury in apoE4 mice. Notably, apoE4-isoform-dependent changes were limited to the hippocampus, in which an inverse correlation of microglial activation with injured volume reduction was identified. Considering that glia play critical roles in damage repair and synaptogenesis [19], our findings suggest that increased early glial activities upon hippocampal injury in apoE4 mice are not efficient for enhancing injury recovery. Impaired glial functions in the presence of the apoE4 allele led to decreased phagocytic capacity and an inability to efficiently clear amyloid β proteins and lipid debris [25, 26]. Higher proinflammatory cytokine release in response to inflammatory stimuli (e.g., lipopolysac-

charide injection) has been observed in apoE4 mice [27]. A recent study, in which microglia depletion was induced in P301S/apoE4 mice, provided strong evidence that enhanced microglial activation in apoE4 mice mediates neurodegeneration [28], consistent with our findings showing an inverse correlation between markers of microglial activities and injury volume reduction. However, to clearly determine whether early activation and recruitment of inflammatory responses have adverse effects in hippocampal injury the additional studies are needed with control of inflammatory activities.

Studies are lacking concerning the region-specific effects of the apoE4–head injury interaction. Mechanical cortical injury in apoE4 transgenic mice has been shown to result in marked alterations of gene expression related to inflammation and cell growth with poor recovery in the hippocampus, compared with other brain regions [7]. However, these results were not supported by a subsequent similar study that used a more physiologically relevant model of apoE KI mice [11]. Although a single focal injury model can replicate practical brain trauma, it is not ideal for making a direct comparison between discrete regions because the affected region receives direct impact, while distant regions are indirectly affected. Our study was unique in that comparisons between hippocampal and cortical focal injury were made by introducing simultaneous injuries into two regions to evaluate the effects of apoE4, permitting the clear identification of increased susceptibility of the hippocampus to apoE4-related altered and enhanced glial activities, as well as diminished injury repair. The regional difference could be exerted by the phenotypical heterogeneity of microglia across different brain regions at least partly [29]. In regards to this issue the subsequent study is necessary which delicately examine apoE4- and region-specific microglial signatures in our models. The neurodegeneration-prone effects of the hippocampus in apoE4 carriers after head trauma are likely to contribute to increased cognitive sequelae, such as poor memory performance after head trauma [4, 5].

Taken together, the results of this study suggest that a comprehensive strategy for modulating inflammatory cell responses in the hippocampus could be a potential strategy to reduce cognitive complications associated with the apoE4 allele.

ACKNOWLEDGEMENTS

This work was supported by Basic Science Research Program (NRF-2018R1A2B6009439 and 2019R1A5A2026045) and the Original Technology Research Program for Brain Science (NRF-2018M3C7A1056293) of the National Research Foundation of Korea funded by the Korean government, MSIT. The funders had no role in study design, data collection and analysis, decision to publish, or preparation of the manuscript.

REFERENCES

1. Wang H, Eckel RH (2014) What are lipoproteins doing in the brain? Trends Endocrinol Metab 25:8-14.
2. Hu J, Liu CC, Chen XF, Zhang YW, Xu H, Bu G (2015) Opposing effects of viral mediated brain expression of apolipoprotein E2 (apoE2) and apoE4 on apoE lipidation and Aβ metabolism in apoE4-targeted replacement mice. Mol Neurodegener 10:6.
3. Teter B (2004) ApoE-dependent plasticity in Alzheimer's disease. J Mol Neurosci 23:167-179.
4. Crawford FC, Vanderploeg RD, Freeman MJ, Singh S, Waisman M, Michaels L, Abdullah L, Warden D, Lipsky R, Salazar A, Mullan MJ (2002) APOE genotype influences acquisition and recall following traumatic brain injury. Neurology 58:1115-1118.
5. Kassam I, Gagnon F, Cusimano MD (2016) Association of the APOE-ε4 allele with outcome of traumatic brain injury in children and youth: a meta-analysis and meta-regression. J Neurol Neurosurg Psychiatry 87:433-440.
6. Chamelian L, Reis M, Feinstein A (2004) Six-month recovery from mild to moderate traumatic brain injury: the role of APOE-epsilon4 allele. Brain 127(Pt 12):2621-2628.
7. Crawford F, Wood M, Ferguson S, Mathura V, Gupta P, Humphrey J, Mouzon B, Laporte V, Margenthaler E, O'Steen B, Hayes R, Roses A, Mullan M (2009) Apolipoprotein E-genotype dependent hippocampal and cortical responses to traumatic brain injury. Neuroscience 159:1349-1362.
8. Mannix RC, Zhang J, Park J, Zhang X, Bilal K, Walker K, Tanzi RE, Tesco G, Whalen MJ (2011) Age-dependent effect of apolipoprotein E4 on functional outcome after controlled cortical impact in mice. J Cereb Blood Flow Metab 31:351-361.
9. Jankowsky JL, Zheng H (2017) Practical considerations for choosing a mouse model of Alzheimer's disease. Mol Neurodegener 12:89.
10. Cao J, Gaamouch FE, Meabon JS, Meeker KD, Zhu L, Zhong MB, Bendik J, Elder G, Jing P, Xia J, Luo W, Cook DG, Cai D (2017) ApoE4-associated phospholipid dysregulation contributes to development of Tau hyper-phosphorylation after traumatic brain injury. Sci Rep 7:11372.
11. Castranio EL, Mounier A, Wolfe CM, Nam KN, Fitz NF, Letronne F, Schug J, Koldamova R, Lefterov I (2017) Gene co-expression networks identify Trem2 and Tyrobp as major hubs in human APOE expressing mice following traumatic

brain injury. Neurobiol Dis 105:1-14.
12. Ben-Moshe H, Luz I, Liraz O, Boehm-Cagan A, Salomon-Zimri S, Michaelson D (2020) ApoE4 exacerbates hippocampal pathology following acute brain penetration injury in female mice. J Mol Neurosci 70:32-44.
13. Giarratana AO, Zheng C, Reddi S, Teng SL, Berger D, Adler D, Sullivan P, Thakker-Varia S, Alder J (2020) APOE4 genetic polymorphism results in impaired recovery in a repeated mild traumatic brain injury model and treatment with Bryostatin-1 improves outcomes. Sci Rep 10:19919.
14. Yang H, An J, Choi I, Lee K, Park SM, Jou I, Joe EH (2020) Region-specific astrogliosis: differential vessel formation contributes to different patterns of astrogliosis in the cortex and striatum. Mol Brain 13:103.
15. Foley KE, Garceau DT, Kotredes KP, Carter GW, Sasner M, Howell GR (2020) *APOE*$^{\varepsilon 3/\varepsilon 4}$ and *APOE*$^{\varepsilon 4/\varepsilon 4}$ genotypes drive unique gene signatures in the cortex of young mice. bioRxiv. 2020. doi: 10.1101/2020.10.28.359422.
16. Piedrahita JA, Zhang SH, Hagaman JR, Oliver PM, Maeda N (1992) Generation of mice carrying a mutant apolipoprotein E gene inactivated by gene targeting in embryonic stem cells. Proc Natl Acad Sci U S A 89:4471-4475.
17. Benjamini Y, Hochberg Y (1995) Controlling the false discovery rate: a practical and powerful approach to multiple testing. J R Stat Soc Series B Stat Methodol 57:289-300.
18. Boyles JK, Pitas RE, Wilson E, Mahley RW, Taylor JM (1985) Apolipoprotein E associated with astrocytic glia of the central nervous system and with nonmyelinating glia of the peripheral nervous system. J Clin Invest 76:1501-1513.
19. Lee E, Chung WS (2019) Glial control of synapse number in healthy and diseased brain. Front Cell Neurosci 13:42.
20. Jeong HK, Ji K, Min K, Joe EH (2013) Brain inflammation and microglia: facts and misconceptions. Exp Neurobiol 22:59-67.
21. Apostolova LG, Risacher SL, Duran T, Stage EC, Goukasian N, West JD, Do TM, Grotts J, Wilhalme H, Nho K, Phillips M, Elashoff D, Saykin AJ; Alzheimer's Disease Neuroimaging Initiative (2018) Associations of the top 20 Alzheimer disease risk variants with brain amyloidosis. JAMA Neurol 75:328-341.
22. Fleminger S, Oliver DL, Lovestone S, Rabe-Hesketh S, Giora A (2003) Head injury as a risk factor for Alzheimer's disease: the evidence 10 years on; a partial replication. J Neurol Neurosurg Psychiatry 74:857-862.
23. Arnold SE, Hyman BT, Flory J, Damasio AR, Van Hoesen GW (1991) The topographical and neuroanatomical distribution of neurofibrillary tangles and neuritic plaques in the cerebral cortex of patients with Alzheimer's disease. Cereb Cortex 1:103-116.
24. Roussarie JP, Yao V, Rodriguez-Rodriguez P, Oughtred R, Rust J, Plautz Z, Kasturia S, Albornoz C, Wang W, Schmidt EF, Dannenfelser R, Tadych A, Brichta L, Barnea-Cramer A, Heintz N, Hof PR, Heiman M, Dolinski K, Flajolet M, Troyanskaya OG, Greengard P (2020) Selective neuronal vulnerability in Alzheimer's disease: a network-based analysis. Neuron 107:821-835.e12.
25. Chung WS, Verghese PB, Chakraborty C, Joung J, Hyman BT, Ulrich JD, Holtzman DM, Barres BA (2016) Novel allele-dependent role for APOE in controlling the rate of synapse pruning by astrocytes. Proc Natl Acad Sci U S A 113:10186-10191.
26. Lin YT, Seo J, Gao F, Feldman HM, Wen HL, Penney J, Cam HP, Gjoneska E, Raja WK, Cheng J, Rueda R, Kritskiy O, Abdurrob F, Peng Z, Milo B, Yu CJ, Elmsaouri S, Dey D, Ko T, Yankner BA, Tsai LH (2018) APOE4 causes widespread molecular and cellular alterations associated with Alzheimer's disease phenotypes in human iPSC-derived brain cell types. Neuron 98:1141-1154.e7.
27. Zhu Y, Nwabuisi-Heath E, Dumanis SB, Tai LM, Yu C, Rebeck GW, LaDu MJ (2012) APOE genotype alters glial activation and loss of synaptic markers in mice. Glia 60:559-569.
28. Shi Y, Manis M, Long J, Wang K, Sullivan PM, Remolina Serrano J, Hoyle R, Holtzman DM (2019) Microglia drive APOE-dependent neurodegeneration in a tauopathy mouse model. J Exp Med 216:2546-2561.
29. Masuda T, Sankowski R, Staszewski O, Böttcher C, Amann L, Sagar, Scheiwe C, Nessler S, Kunz P, van Loo G, Coenen VA, Reinacher PC, Michel A, Sure U, Gold R, Grün D, Priller J, Stadelmann C, Prinz M (2019) Spatial and temporal heterogeneity of mouse and human microglia at single-cell resolution. Nature 566:388-392.